

# Fabrication of a Large-aspect-ratio Single-thread Helical Electrode using Multiple Wire Electrochemical Micromachining

Xiaolong Fang\*, Tao Yang, Mi Chen, Di Zhu

National Key Laboratory of Science and Technology on Helicopter Transmission, Nanjing University of Aeronautics and Astronautics, Nanjing 210016, China

\*E-mail: [xlfang@nuaa.edu.cn](mailto:xlfang@nuaa.edu.cn)

Received: 19 February 2020 / Accepted: 12 May 2020 / Published: 10 July 2020

---

Helical electrode is known to be effective in accelerating the renewal of fresh electrolyte and the removal of electrolysis products in wire electrochemical machining. To cut macroscopic structures such as slots in a turbine disc, this type of machining requires a large-aspect-ratio helical electrode with a diameter as small as 0.5 mm and a spiral length of around 40 mm. However, fabricating helical electrode has invariably been difficult at large aspect ratio. This paper proposes using multiple wire electrochemical micromachining to fabricate a large-aspect-ratio single-thread helical electrode. The machining procedure is to (i) arrange  $n$  metallic wires in a row with an adjacent interval  $\delta$  that equals the thread pitch  $S$ , (ii) perform multiple wire electrochemical machining for one revolution, then (iii) move the tool to the next position with a distance  $(n-1)S$  away and wait for another machining cycle. Thus, the head and tail of neighbouring thread grooves machined by two different wire electrodes are connected, and a large-aspect-ratio threaded helical electrode is obtained highly efficiently. Experiments are conducted to investigate how the groove size is affected by the electrolyte concentration and the amplitude, frequency and duty ratio of the pulsed voltage, and the results show that groove localization and edge roundness are affected most by the electrolyte concentration and the pulsed-voltage amplitude and duty ratio. With the optimal parameters of a pulsed voltage of 11 V in amplitude, 25% in duty ratio and 100 kHz in frequency and a 15-g/L sodium nitrate solution, a single-thread helical electrode with textured sharp grooves of 498.2  $\mu\text{m}$  in width, 168.8  $\mu\text{m}$  in depth and 20 mm in spiral length was fabricated. Finally, the feasibility of this single-thread helical electrode was verified by electrochemical machining a complex structure in a 20-mm-thick block.

---

**Keywords:** Wire electrochemical micromachining, Groove, Helical electrode, Large aspect ratio

## 1. INTRODUCTION

Helical tools are used to good effect in mechanical drilling, electro-discharge drilling [1] and electrochemical drilling [2,3] because of their excellent performance at removing products via the spiral

microgrooves on their surfaces. Recently, they have begun to be used in wire electrochemical machining (WECM). Fang et al. [4] used a helical drill of 0.3 mm in diameter as the electrode with which to fabricate a complex hollow structure, and Klocke et al. [5] twisted two brass wires together as a double-helix electrode of 0.5 mm in diameter. Combined with rotation, these helical tools have been shown to be effective in accelerating the renewal of fresh electrolyte and the removal of electrolysis products, thereby enhancing the machining rate considerably. To cut macroscopic structures such as fir-tree slots in a turbine disc, WECM requires the electrode diameter to be as small as 0.5 mm and its spiral length to be around 40 mm.

However, fabricating helical electrode has invariably been difficult at large aspect ratio. Mechanical grinding encounters severe deformation due to poor wire stiffness [6]. Wire electro-discharge grinding [7] and electrolytic in-process dressing grinding [8] can produce staged microscopic pins or rods with a maximum aspect ratio of 30, but they are not good at generating continuous grooves on a wire surface. Electrochemical micromachining (ECMM), which is a contactless machining method that involves removing material via controlled electrochemical reactions, has outstanding characteristics in microscopic fabrication, such as being free of cutting forces and residual stresses and leaving a good surface finish [9]. ECMM has been used widely to prepare microscopic electrode via various methods. Lim et al. [10] etched a rod of 50  $\mu\text{m}$  in diameter with an aspect ratio of 80 by regulating the current density. Wang et al. [11] fabricated microscopic pins with a diameter of several hundred nanometres and aspect ratios up to 70 using liquid-membrane electrochemical etching. Han and Kunieda [12] machined tungsten microscopic rods in wire electrochemical grinding using a sodium nitrate solution and a bipolar current. However, the aforementioned methods are unfortunately not suitable for fabricating helical grooves on a large-aspect-ratio rod.

Wire ECMM (WECMM), which uses a metallic wire with a diameter of microns as the cathode, is a branch of ECMM. By applying current in ultra-short pulses, microstructures such as microscopic gears and grooves have been fabricated successfully [13–15]. Liu et al. [16] used a tungsten wire of 20  $\mu\text{m}$  in diameter as the electrode and made micro-tools of various shapes (e.g. semi-cylinder, thin slice, triangular prism) from a rod of 300  $\mu\text{m}$  in diameter. Xu et al. [17] used a tungsten wire of 10  $\mu\text{m}$  in diameter and fabricated square columnar tools with a section size of 10  $\mu\text{m} \times 10 \mu\text{m}$ . When the workpiece is mounted on a spindle and rotates in the machining process, various axisymmetric structures as well as grooves can be produced with a numerically controlled feed motion of the wire electrode in WECMM. El-Taweel and Gouda [18] used a copper wire as the electrode for wire electrochemical turning (WECT) and investigated how the process parameters influenced the material removal rate (MRR) and circular groove size. Haridy et al. [19] presented an integrated framework combining design of experiments and statistical process control to understand the WECT process. Zou et al. [20] used a 100- $\mu\text{m}$  molybdenum wire as the electrode and fabricated ribbed grooves of 113  $\mu\text{m}$  in width and 100  $\mu\text{m}$  in depth on a 500- $\mu\text{m}$  stainless-steel rod, which was then used for the electrochemical cutting of a 20-mm-thick block. Wang et al. [21] used a 20- $\mu\text{m}$  tungsten wire and machined microscopic annular grooves with a width of 100  $\mu\text{m}$ , a pitch of 80  $\mu\text{m}$  and a depth of 100  $\mu\text{m}$  on an aluminium rod with a diameter of 3 mm. Sharma et al. [22] used WECMM to generate thread profiles on cylindrical shafts made of Ti-6Al-4V, 304 stainless steel and copper. To obtain a sharp thread profile, they stuck a mask made of polyamide sheet on the shaft surface to prevent stray current attack.

Having multiple electrode working at different stations simultaneously could significantly increase the machining efficiency of arrayed structures. Patel et al. [23] clubbed thin copper sheets together as the electrode and fabricated micro-channels on a hypodermic needle of 1200 μm in diameter. In WECMM, metallic wires are usually mounted on a specific fixture in parallel and fed together to the workpiece [24–26]. How the number of wire electrodes affects the machining accuracy and maximum electrode feed rate has been investigated. However, although work has been done on generating grooves [20–22] and arrayed features [24–26] using WECM, there is little literature that assesses multiple wire electrochemical machining (M-WECM) of helical grooves on a large-aspect-ratio cylindrical surface. The present aim is to use multiple wire electrode to produce single-thread spiral grooves at each pitch simultaneously, whereupon the head and tail of two neighbouring grooves will be connected to form a large-aspect-ratio single-thread helical electrode highly efficiently. How the electrolyte concentration and the voltage amplitude, frequency and pulse duty ratio (PDR) affect the groove size is investigated to obtain uniformly distributed sharp grooves. Finally, the feasibility of a self-made large-aspect-ratio electrode is investigated experimentally for the electrochemical machining of a 20-mm-thick structure.

## 2. EXPERIMENTAL DETAILS

Figure 1 shows a schematic of the WECM of a rod for a threaded electrode. Each end of the rod is restricted by a guide, with the upper end connected to a reducer driven by a motor. The rod is also connected electrically to the positive terminal of a pulse generator via a specific brush.

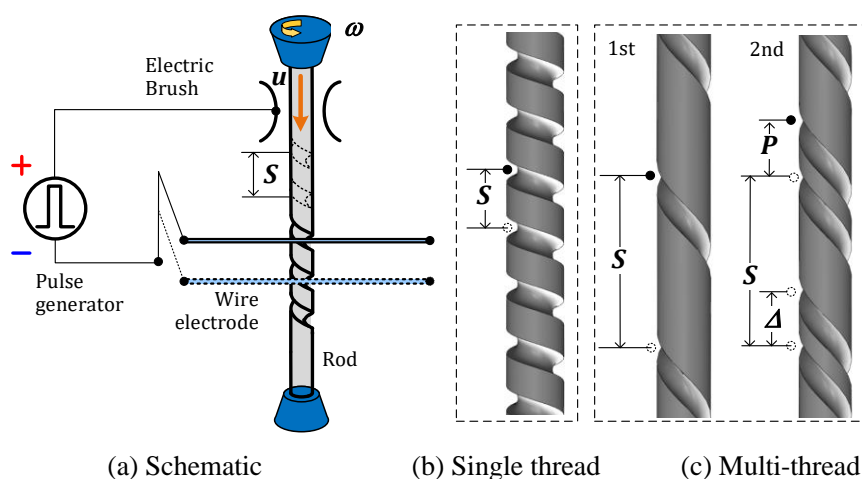


**Figure 1.** Schematic of producing threaded wire electrode via wire electrochemical machining.

First, the wire electrode is fed to the rod horizontally and material starts dissolving to generate a shallow groove on the rod surface. Once the wire electrode reaches a specific depth, namely the groove depth, the cylindrical rod starts to rotate and move slowly in its axial direction. A spiral groove known as a single-thread helix then forms gradually on the rod surface. From the kinematics, the thread pitch  $S$  can be calculated as

$$S = 2\pi u / \omega = 60u / n_r, \tag{1}$$

where  $u$  is the feed rate of the rod in its axial direction,  $\omega$  is the angular velocity and  $n_r$  is the rotation speed of the rod. If a multi-thread with a lead  $P$  and a thread number  $n$  is required, then the wire electrode could start several repetitive grooving processes from different positions with a contiguous interval  $\Delta$  that equals the thread lead  $P$ . However, producing a large-aspect-ratio threaded electrode that way would take a long time.

Using multiple wire electrodes would significantly increase the machining efficiency of arrayed structures. If multiple metallic wires are arranged in a row and mounted on a specific clamping apparatus as a tool cathode, the large-aspect-ratio rod could be processed simultaneously at different pitches or leads, as shown in Figure 2. Before machining, the spatial position of the multiple wire electrodes is adjusted to ensure that each wire has the same initial distance to the rod surface and the multiple wire electrodes are together immersed in the electrolyte bulk.

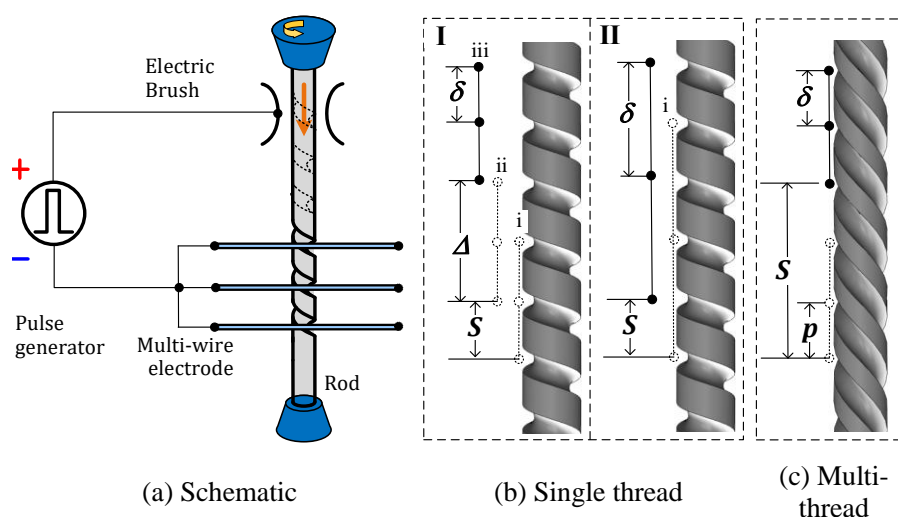


**Figure 2.** Schematic of producing threaded electrode via three-wire electrochemical machining.

There are two procedures for obtaining a single-thread helical electrode by using multiple wire electrodes. Procedure I is as follows: (i) arrange  $n$  metallic wires in a row with an adjacent interval  $\delta$  that equals  $S$ , (ii) maintain M-WECM for one revolution, then (iii) move the wire electrodes to the next position a distance  $\Delta_I$  away and wait for the next machining cycle. The distance  $\Delta_I$  equals  $(n-1)S$ . Thus, the head and tail of two neighbouring thread grooves machined by different wire electrodes are connected, and a large-aspect-ratio threaded helical electrode is obtained.

Procedure II is as follows: (i) arrange  $n$  metallic wires in a row with an adjacent interval  $\delta$  that equals an integer multiple of the thread pitch (i.e.  $mS$ ), (ii) maintain M-WECM for  $m$  rotations, then (iii) move the wire electrodes to the next position a distance  $\Delta_{II}$  away and wait for the next machining cycle. The distance  $\Delta_{II}$  equals  $(n-1)mS$ . Thus, the head and tail of two neighbouring thread grooves with  $m$  loops are connected.

To obtain a multi-thread helical electrode with a thread number  $k$ , the machining procedure is to arrange  $k$  metallic wires in a row with an adjacent interval  $S$  and maintain M-WECM until the required spiral length is achieved.

In this study, we focus on improving the machining efficiency of a large-aspect-ratio single-thread helical electrode, and the machining procedure is carried out according to procedure I. When the pitch and the rod feed rate are chosen as 1 mm and 0.2  $\mu\text{m/s}$ , respectively, the rod rotates quite slowly. Because the rotation speed of a servo motor is usually less than 3000 rpm, the reduction ratio of the reducer is set as large as 200,175. Table 1 lists the corresponding relationship between pitch and motor speed. In this research, the required pitch is 1.00 mm and the motor speed is chosen as 2400 rpm.

**Table 1.** Thread pitch vs. motor speed.

$n_m$ [rpm]	$p$ [mm]
800	2.00
1600	1.50
2000	1.20
2400	1.00

Figure 3 shows the self-developed experimental setup for the WECM of a threaded helical electrode. This apparatus includes an X–Y linear motion stage, a Z linear axis, a low-speed rotation module, a multiple wire clamping fixture, an electrolyte unit (not shown), a pulse generator and an oscilloscope. The low-speed rotation module containing a servo motor and a harmonic reducer is installed on the Z axis. Furthermore, a charge-coupled device is used to adjust the initial tool position and observe the machining process. In the experiments, tungsten wires of 100  $\mu\text{m}$  in diameter were used as the multiple wire electrodes, and a stainless-steel rod of 500  $\mu\text{m}$  in diameter acted as the workpiece. The multiple wire clamping fixture could hold 10 wires in parallel with an interval of 1 mm. To obtain a helical electrode with a pitch of 1 mm and a spiral length of 20 mm, we used 10 wires with an interval of 1 mm to produce a spiral length of 10 mm in one revolution and then moved them to the next 10-mm length.

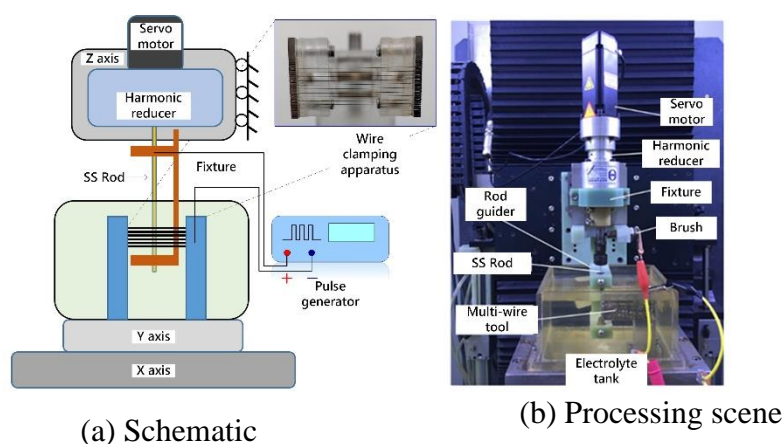


**Figure 3.** Experimental setup for the wire electrochemical micromachining of a helical electrode.

In electrochemical machining, a pulsed current and low-concentration electrolyte are usually used to obtain high accuracy and localized dissolution. In the present study, experiments were carried

out to investigate how typical parameters influence the groove geometry. The main WECM parameters were chosen through experimental trials and subsequently measured using a microscope (OLS4100; Olympus, Japan). Because a picture with the required resolution could contain only three grooves, the centre three grooves of the 10 were measured. As shown in Figure 4, each groove was measured three times at different positions to obtain an average value of the groove width along its axial direction.

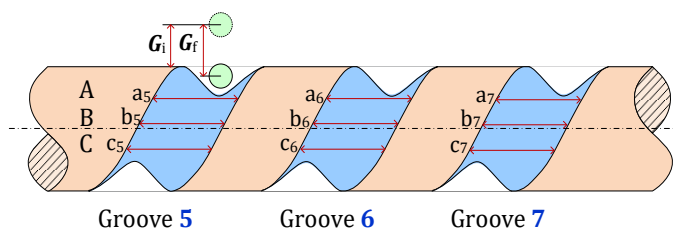


**Figure 4.** Measurement of groove size.

### 3. RESULTS AND DISCUSSION

#### 3.1 Multi-groove size consistency

First, the feasibility of using multiple wire ECM (M-WECM) to cut grooves in a slender rod was evaluated experimentally in a 15-g/L sodium nitrate electrolyte. The pulsed voltage was 13 V in amplitude, 18% in PDR and 100 kHz in frequency. Figure 5 shows the groove-width distribution with different feed depths  $G_f$  increasing from 0.15 mm to 0.20 mm. The results show that the groove width increases with the initial feed depth. The standard deviations of the groove widths of these 10 grooves are 16.85  $\mu\text{m}$ , 30.59  $\mu\text{m}$  and 29.92  $\mu\text{m}$ , respectively. When the feed depth is 0.15 mm, the groove-width range is 53  $\mu\text{m}$ . The results indicate that the proposed method is feasible for fabricating multi-grooves on a large-aspect-ratio rod with high consistency. Therefore, a feed depth of 0.15 mm was used in the following experiments.

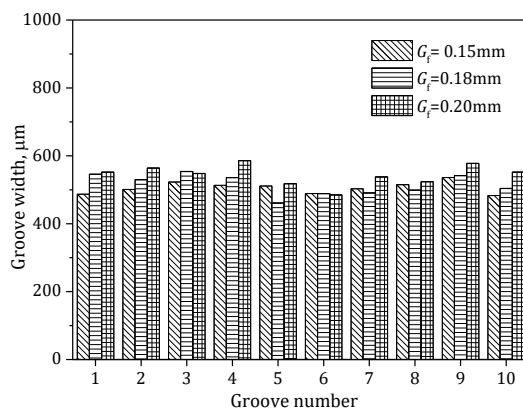


**Figure 5.** Variation of groove-width consistency (voltage amplitude: 13 V; pulse duty ratio (PDR): 18%; frequency: 100 kHz; electrolyte concentration: 15-g/L).

### 3.2 Effect of voltage amplitude

This set of experiments was conducted to evaluate how the amplitude of the applied voltage influences the groove shaping in M-WECMM. The pulsed voltage was 25% in PDR and 100 kHz in frequency, and the electrolyte was 15-g/L sodium nitrate at 28°C. Single-thread grooves machined with different voltage amplitudes are shown in Figure 6, and the measured average groove width is shown in Figure 7. The results show that the size of the three adjacent grooves was highly consistent and increased gradually with the voltage amplitude. Sharma et al. [27] and Xu et al. [25] also indicated that increasing the voltage amplitude would widen the grooves. When the voltage is lower than 10 V, short circuits happened frequently in the experiments because the resultant feed rate of the rod combining rotation and axial feed was higher than the MRR. For voltages above 11 V, most of the material on the wire surface was dissolved and the groove width was more than half of the single-thread groove pitch. This shows that excessive material was removed and that the machined groove suffered over current action. This may weaken the tool stiffness while also lessening the efficacy of the rotation of the helical electrode at perturbing the electrolyte flow in WECM. For voltages between 10 V and 11 V, the groove width and profile exhibit no obvious differences. Here, an amplitude of 11 V is recommended.

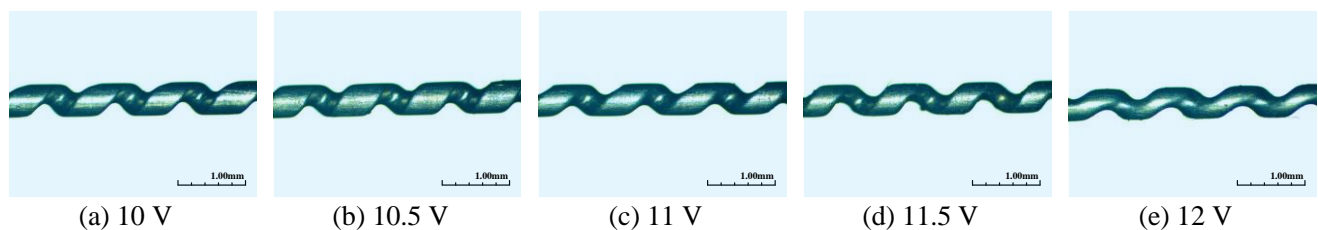


**Figure 6.** Grooves machined with different voltages (PDR: 25%; frequency: 100 kHz; electrolyte concentration: 15-g/L).

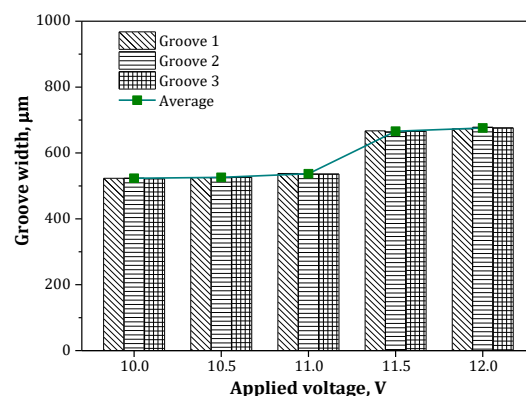


**Figure 7.** Variation of groove width with voltage amplitude (PDR: 25%; frequency: 100 kHz; electrolyte concentration: 15-g/L).

### 3.3 Effect of pulse duty ratio

This set of experiments was conducted to evaluate how the PDR affects the multi-groove shaping process. The pulsed voltage was 11 V in amplitude and 100 kHz in frequency, and the electrolyte was 15-g/L sodium nitrate at 28°C. Figure 8 shows grooves machined with different PDRs, and how their

average widths varied is plotted in Figure 9. The results show that the groove size increased gradually with increasing PDR. Yu et al. [28] and Shin et al. [29] also obtained this trend through experiments. A larger PDR means more pulse on time and more electrical energy applied for material removal. When the PDR exceeds 30%, the groove edges are rounded and the grooves are more than 0.6 mm wide, which is not suitable for accelerating the electrolyte flow in the WECM of macroscopic structures. Furthermore, when the PDR is less than 15%, the MRR drops below the rod's resultant feed rate, resulting in occasional short circuits. Therefore, a PDR of 25% is recommended for the M-WECMM of a helical electrode.

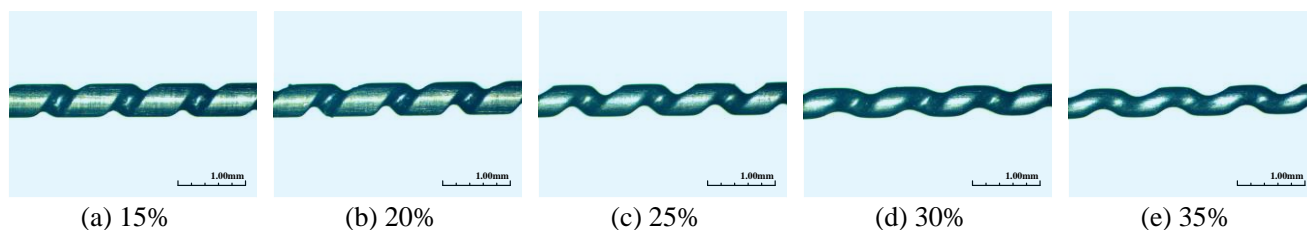


**Figure 8.** Grooves machined with different PDRs (voltage amplitude: 11 V; frequency: 100 kHz; electrolyte concentration: 15-g/L).

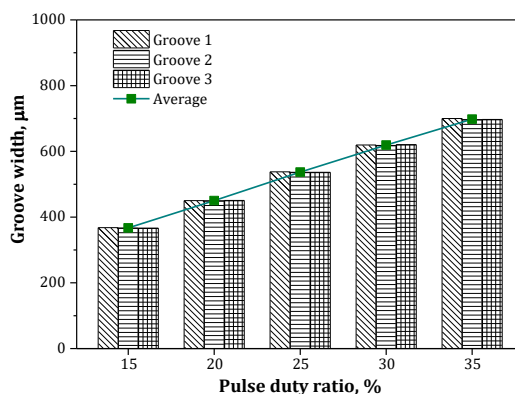


**Figure 9.** Variation of groove width with voltage PDR (voltage amplitude: 11 V; frequency: 100 kHz; electrolyte concentration: 15-g/L).

### 3.4 Effect of pulse frequency

This set of experiments was conducted to evaluate how the voltage pulse frequency affects the helical groove shaping in M-WECMM. The pulsed voltage was 11 V in amplitude and 25% in PDR, and the electrolyte was 15-g/L sodium nitrate at 28°C. Figure 10 shows grooves machined with different pulse frequencies, and how their widths varied is shown in Figure 11. The results show that when the frequency is decreased from 100 kHz to 50 kHz, the grooves become slightly wider but the groove edge becomes rounded quickly. When the frequency is 20 kHz, the grooves are wider than 0.7 mm and the required helical electrode is more like a helix coil, which would certainly be unable to perturb the electrolyte flow to generate rapid renewal. As is well known, a lower pulse frequency means more effective machining time in a pulse duration, thereby leading to more material removal and larger groove

size. When the pulse duration is short enough, the electric circuit charging time will occupy a non-negligible proportion and the material dissolution localization will be confined to produce sharp edges. Qu et al. [30] and Koyano et al. [31] also found that increasing the pulse frequency can improve the accuracy of electrochemical machining. Consequently, a pulse frequency of 100 kHz is advised for obtaining chiselled helical grooves on a large-aspect-ratio helical electrode.

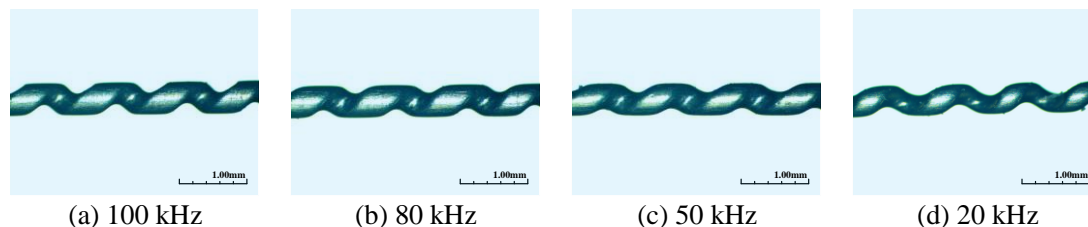


**Figure 10.** Grooves machined with different pulse frequencies (voltage amplitude: 11 V; PDR: 25%; electrolyte concentration: 15-g/L).

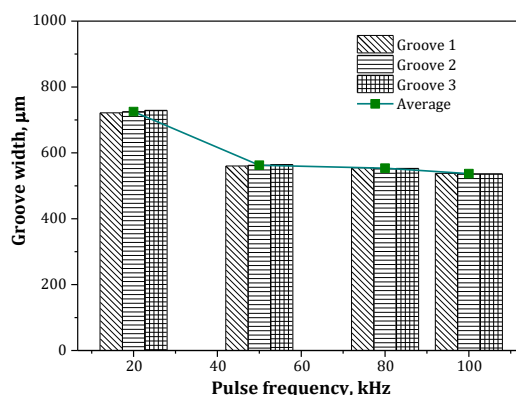


**Figure 11.** Variation of groove width with pulsed voltage frequency (voltage amplitude: 11 V; PDR: 25%; electrolyte concentration: 15-g/L).

### 3.5 Effect of electrolyte concentration

This set of experiments was conducted to evaluate how the electrolyte concentration influences the groove geometry in M-WECMM. The pulsed voltage was 11 V in amplitude, 25% in PDR and 100 kHz in frequency. Figure 12 shows grooves machined with different electrolyte concentrations, which varied from 15 g/L to 35 g/L with an interval of 5 g/L. This shows that the grooves had poor geometry and that their edges became rounded as the concentration increased. Higher electrolyte concentration means higher electric conductivity, which results in increased current density and MRR. Consequently, a low electrolyte concentration is preferable to obtain a clear-cut groove edge. However, when the concentration is decreased below 15 g/L, the MRR will be lower than the rod resultant feed rate, thereby causing occasional short circuits. Furthermore, the groove width increases quickly with increasing electrolyte concentration, as plotted in Figure 13, which is similar to the conclusion by Yang et al. [32]

and Meng et al. [33]. The groove width exceeded 0.6 mm when the concentration reached 25 g/L. Therefore, a 15-g/L sodium nitrate electrolyte is recommended.

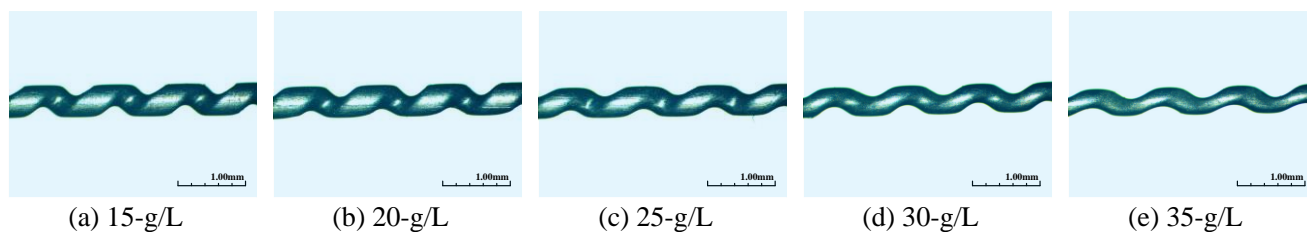


**Figure 12.** Grooves machined with different electrolyte concentrations (voltage amplitude: 11 V; PDR: 25%; frequency: 100 kHz).

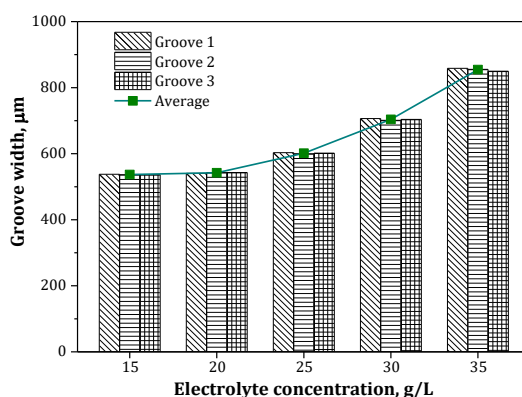


**Figure 13.** Variation of groove width with electrolyte concentration (voltage amplitude: 11 V; PDR: 25%; frequency: 100 kHz).

### 3.6 Application of this fabricated helical electrode

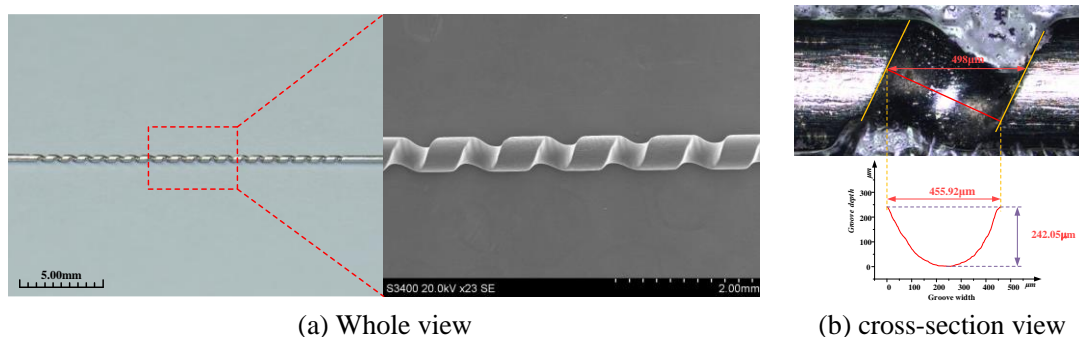


**Figure 14.** Helical electrode machined under optimal conditions (voltage amplitude: 11 V; PDR: 25%; frequency: 100 kHz; electrolyte concentration: 15-g/L).

A large-aspect-ratio single-thread helical electrode with sharp grooves of 498.2 µm in width, 168.8 µm in depth and 20 mm in spiral length was fabricated under the optimal parameters of a pulsed

voltage of 11 V in amplitude, 25% in PDR and 100 kHz in frequency, and a 15-g/L sodium nitrate electrolyte. Figure 14 shows a photograph of the electrode and an enlarged scanning-electron-microscopy picture of the helical groove. It can be seen that the grooves had sharp edges and good size consistency all along the length.

Afterwards, this helical electrode was used for the electrochemical machining of macroscopic structures in a block made of 304 stainless steel, as illustrated in Figure 15(a). The machining conditions were a pulsed voltage of 18 V in amplitude, 30% in PDR and 100 kHz in frequency. The electrolyte was 80-g/L sodium nitrate solution at 28°C. The helical electrode was mounted on a spindle and rotated at a speed of 5000 rpm. In the machining, the helical electrode was fed simultaneously at 2 μm/s along a programmed trajectory. A tree-like structure of 10 mm in thickness with a kerf width is 623.1 μm was machined stably as shown in Figure 15. A dodecagonal structure of 20 mm in thickness was also fabricated, and the surface roughness Ra was only 0.602 μm. Furthermore, when the threaded helical electrode was made unsymmetrical or with a lapped tool mark due to an eccentricity error, the surface of the machined macroscopic structure was corrugated as shown in Figure 16.

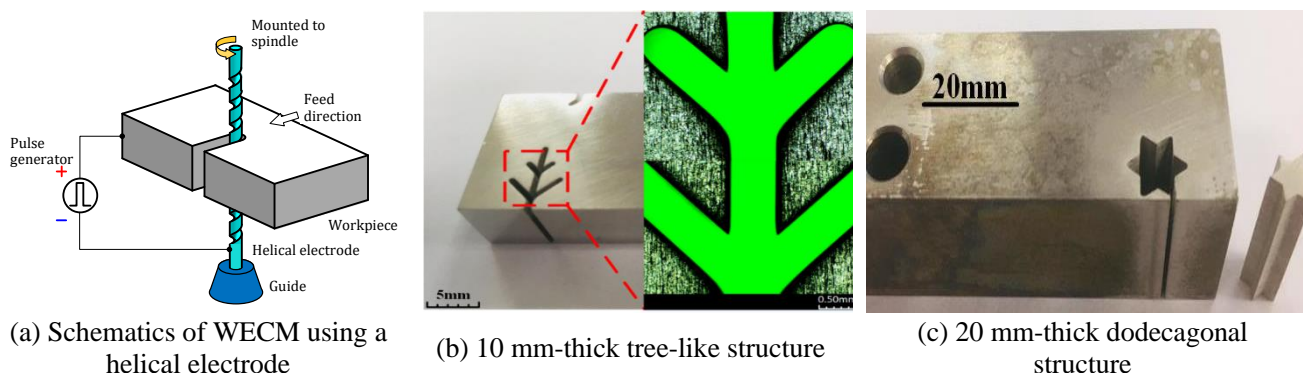


**Figure 15.** Macroscopic structure machined with the machined electrode in WECM (voltage amplitude: 18 V; PDR: 30%; frequency: 100 kHz; electrolyte concentration: 80-g/L; spindle speed: 5000 rpm).

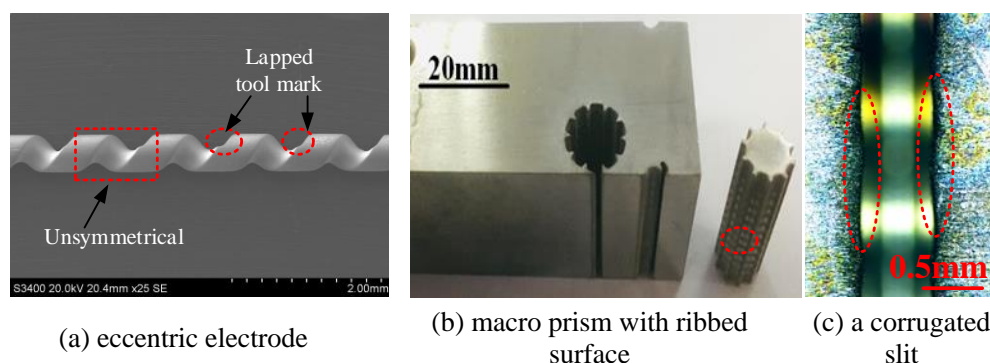


**Figure 16.** Eccentric electrode and corresponding machined surface (voltage amplitude: 18 V; PDR: 30%; frequency: 100 kHz; electrolyte concentration: 80-g/L; spindle speed: 5000 rpm).

#### 4. CONCLUSIONS

This paper proposed a method for the M-WECMM of a large-aspect-ratio single-thread helical electrode. The conclusions are as follows.

1. The method could fabricate multi-grooves on a large-aspect-ratio rod with high consistency. The voltage amplitude, PDR and the electrolyte concentration had more-significant influences on groove localization and edge geometry than did the voltage amplitude and pulse frequency.
2. A single-thread helical electrode textured with sharp grooves of 498.2  $\mu\text{m}$  in width, 168.8  $\mu\text{m}$  in depth and 20 mm in spiral length was fabricated with the optimal parameters of a pulsed voltage of 11 V in amplitude, 25% in PDR and 100 kHz in frequency in a 15-g/L sodium nitrate solution.
3. A dodecagonal structure with a thickness of 20 mm was machined stably in WECM with the prepared large-aspect-ratio helical electrode.

#### ACKNOWLEDGEMENTS

The work was supported by the Joint Funds of the National Natural Science Foundation of China and Guangdong Province (Grant No. U1601201), the National Natural Science Foundation of China for Creative Research Groups (Grant No. 51921003).

#### References

1. J.C. Hung, J.K. Lin, B.H. Yan, H.S. Liu and P.H. Ho, *J. Micromech. Microeng.*, 16 (2006) 2705.
2. H.P. Tsui, J.C. Hung, J.C. You and B.H. Yan, *Mater. Manuf. Process.*, 23 (2008) 499.
3. Y. Liu, M.H. Li, J.R. Niu, S.Z. Lu and Y. Jiang, *Micromachines*, 10 (2019) 28.
4. X.L. Fang, X.H. Zou, P.F. Zhang, Y.B. Zeng and N.S. Qu, *Int. J. Adv. Manuf. Technol.*, 84 (2016) 929.
5. F. Klocke, T. Herrig, M. Zeis and A. Klink, *Procedia CIRP*, 68 (2018) 725.
6. S.Y. Zhang, Z.Q. Liang, X.B. Wang, T.F. Zhou, L. Jiao, P. Yan and H.C. Jian, *Int. J. Adv. Manuf. Technol.*, 86 (2016) 2823.
7. T. Masuzawa and H. Tönshoff, *CIRP Ann.*, 46 (1997) 621.
8. K. Rajurkar, G. Levy, A. Malshe, M. Sundaram, J. McGeough, X. Hu, R. Resnick and A. DeSilva, *CIRP Ann.*, 55 (2006) 643.
9. D.Y. Wang, B. He, W.J. Cao, *Applied Sciences*, 9 (2019) 690.
10. Y.M. Lim, H.J. Lim, J.R. Liu and S.H. Kim, *J. Mater. Process. Technol.*, 141 (2003) 251.
11. Y.F. Wang, N.S. Qu, Y.B. Zeng, X.J. Wu, D. Zhu, *Int. J. Precis. Eng. Manuf.*, 14 (2013) 2179.
12. W. Han and M. Kunieda, *Precis. Eng.*, 52 (2018) 458.
13. B. Kim, C. Na, Y. Lee, D. Choi and C. Chu, *CIRP Ann.*, 54 (2005) 191.
14. D. Zhu, K. Wang and N.S. Qu, *CIRP Ann. Manuf. Technol.*, 56 (2007) 241.
15. Y.B. Zeng, Q. Yu, S.H. Wang and D. Zhu, *CIRP Ann. Manuf. Technol.*, 61 (2012) 195.
16. Z. Liu, Y.B. Zeng and W.B. Zhang, *Adv. Mech. Eng.*, 6 (2014) 382105.
17. K. Xu, Y.B. Zeng, P. Li and D. Zhu, *Precis. Eng.*, 47 (2017) 487.
18. T.A. El-Taweel and S.A. Gouda, *J. Appl. Electrochem.*, 41 (2011) 161.
19. S. Haridy, S.A. Gouda and Z. Wu, *Int. J. Adv. Manuf. Technol.*, 53 (2011) 191.
20. X.H. Zou, X.L. Fang, Y.B. Zeng, P.F. Zhang and D. Zhu, *Int. J. Electrochem. Sci.*, 11 (2016) 2335.
21. X.Y. Wang, X.L. Fang, Y.B. Zeng and N.S. Qu, *Int. J. Electrochem. Sci.*, 11 (2016) 7216.
22. V. Sharma, D.S. Patel, V.K. Jain, J. Ramkumar and A. Tyagi, *J. Electrochem. Soc.*, 165 (2018) E397.

23. D.S. Patel, A. Singh, V. Jain, J. Ramkumar and A. Shrivastava, *Int. J. Adv. Manuf. Technol.*, 100 (2019) 1311.
24. X.L. Fang, P. Li, Y.B. Zeng and D. Zhu, *Procedia CIRP*, 42 (2016) 423.
25. K. Xu, Y.B. Zeng, P. Li, X.L. Fang and D. Zhu, *Int. J. Electrochem. Sci.*, 11 (2016) 5403.
26. H.D. He, Y.B. Zeng, Y.Y. Yao and N.S. Qu, *J. Manuf. Process.*, 25 (2017) 452.
27. V. Sharma, I. Srivastava, V.K. Jain and J. Ramkumar, *Electrochim. Acta*, 312 (2019) 329.
28. N. Yu, X.L. Fang, L.C. Meng, Y.B. Zeng and D. Zhu, *J. Appl. Electrochem.*, 48 (2018) 263.
29. H.S. Shin, B.H. Kim and C.N. Chu, *J. Micromech. Microeng.*, 18 (2008) 075009.
30. N.S. Qu, K. Xu, Y.B. Zeng and Q. Yu, *Int. J. Electrochem. Sci.*, 8 (2013) 12163.
31. T. Koyano and M. Kunieda, *Procedia CIRP*, 6 (2013) 390.
32. T. Yang, Y.B. Zeng, X.L. Fang and Y.L. Li, *Int. J. Electrochem. Sci.*, 15 (2020) 1691.
33. L.C. Meng, Y.B. Zeng and D. Zhu, *Electrochim. Acta*, 233 (2017) 274.

© 2020 The Authors. Published by ESG ([www.electrochemsci.org](http://www.electrochemsci.org)). This article is an open access article distributed under the terms and conditions of the Creative Commons Attribution license (<http://creativecommons.org/licenses/by/4.0/>).